Supporting Information

Boosting Anti-Tumor Immunity with Boron-based Nanosheets via Photodynamic-elicited Pyroptosis and Adjuvant Delivery

Xinran Xie [a,b,d,#], Shuaiyin Zhang [a,b,d,#], Ming Liu [b,d], Yang Ye [b,d], Yongxin Huang [e], Zhixin Li [a,d], Junyan Lin [b,d], Jie Liu [b], Jingchun Zhou [c,*], Changyi Xu [a,b,d,*], Zhaoxu Tu [a,b,d,*]

[a] Guangdong Research Institute of Gastroenterology, The Sixth Affiliated Hospital, Sun Yat-sen University, Guangzhou, Guangdong 510655, China

[b] Department of Otolaryngology, The Sixth Affiliated Hospital, Sun Yat-sen University, Guangzhou, Guangdong 510655, China

[c] Department of Otorhinolaryngology, Shenzhen People's Hospital (The Second Clinical Medical College, Jinan University; The First Affiliated Hospital, Southern University of Science and Technology), Shenzhen 518020, Guangdong, China

[d] Biomedical Innovation Center, The Sixth Affiliated Hospital, Sun Yat-sen University, Guangzhou, Guangdong 510655, China

[e] Guangzhou Municipal and Guangdong Provincial Key Laboratory of Protein Modification and Degradation, School of Basic Medical Sciences, Guangzhou Medical University, Guangzhou, 511436, China

† Electronic supplementary information (ESI) available.

#These authors contributed equally to this work.

*Corresponding authors.

E-mail address: tuzhx@mail.sysu.edu.cn (Zhaoxu Tu); xuchy29@mail2.sysu.edu.cn (Changyi Xu); szhospital@hotmail.com (Jingchun Zhou)

Materials

Magnesium boride (MgB2, catalogue no. 553913), gluconic acid (catalogue No. G1951), 2-morpholinoethanesulfonic acid (MES, catalogue No. M3671), 1-(3-dimethylaminopropyl)-3-ethylcarbodiimide (EDC, catalogue No. E7750), New Indocyanine Green (IR-820, catalogue No. 172616-80-7), and 2′,7′-dichlorofluorescin diacetate (DCFH-DA, catalogue No. D6883) were bought from Sigma-Aldrich (St. louis, USA). Polyethyleneimine, branched, M.W. 1,200 (catalogue No. 9002-98-6) was purchased from Alfa Aesar (Heysham, UK). Loxoribine (catalogue No. 121288-39-9) was purchased from TargetMol Chemicals Inc. (Boston, MA, USA). Phosphate buffered saline (PBS, catalogue No. C10010500BT), DMEM high glucose medium (catalogue No. C11995500BT), fetal bovine serum (FBS, catalogue No. 10099141) and Penicillin/Streptomycin (catalogue No. 15140122) were obtained from GIBCO (Grand Island, USA). Cell counting kit-8 (CCK8, catalogue No. K1018) was provided by APE×BIO (Houston, USA). Calcein/PI Cell Viability/Cytotoxicity Assay Kit (catalogue No. C2015M), Cell Apoptosis Detection Kit with Annexin V-mCherry and SYTOX Green (catalogue No. C1070M), Enhanced ATP Assay Kit (catalogue No. S0027), Hoechst 33342 (catalogue No. C1022), and LDH Cytotoxicity Assay Kit (catalogue No. C0016) were obtained from Beyotime (Shanghai, CHN). Fluorescein (FITC) Tunel Cell Apoptosis Detection Kit (catalogue No. G1501) was purchased from Servicebio (Wuhan, CHN). CST-Anti-rabbit IgG (H+L), F(ab')2 Fragment (Alexa Fluor® 488 Conjugate) (catalogue No. 4412S) and Cleaved Caspase-3 (Asp175) (5A1E) Rabbit mAb (catalogue No. 9664T) were bought from Cell Signaling

Technology (Danvers, MA, USA). Anti-HMGB1 (catalogue No. ab79823) and Anti-DFNA5/GSDME (catalogue No. ab215191) were gained from Abcam (Cambridge, UK). Calreticulin (D3E6) XP® Rabbit mAb (CRT, catalogue No. 12238T) was gained from Sciwaro (Foshan, CHN). The antibodies involved in flow cytometry (details were shown in Table S1) were bought from Biolegend (San Diego, USA).

Table S1. Fluorescent antibodies for flow cytometry

Antibody	Catalogue No.
Zombie Aqua™ Fixable Viability Kit	423101
FITC anti-mouse CD45	103108
PE/Cyanine7 anti-mouse CD11c	117317
APC anti-mouse F4/80	123115
APC anti-mouse CD80	104714
APC/Cyanine7 anti-mouse CD86	105029
Brilliant Violet 421™ anti-mouse I-A/I-E	107632
Brilliant Violet 605™ anti-mouse/human CD11b	101257
PE anti-mouse CD206	141706
PerCP/Cyanine5.5 anti-mouse CD3	100218
APC/Cyanine7 anti-mouse CD4	100414
PE/Cyanine7 anti-mouse CD8a	100722

Supplementary Figures

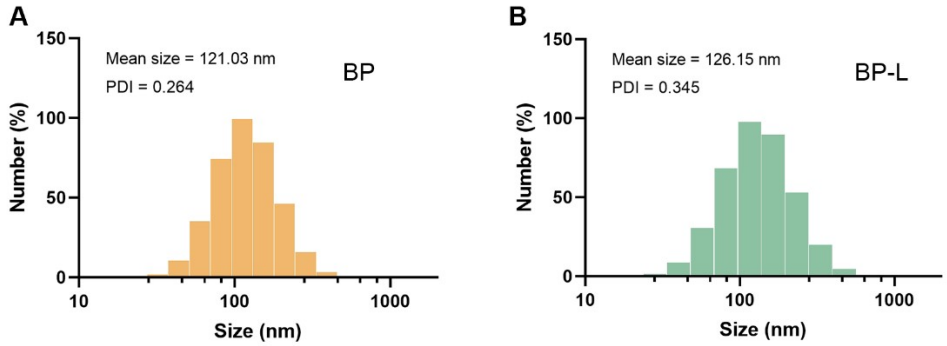

Figure S1. Hydrodynamic diameter of BP and BP-L. (A) Size of BP measured by DLS. (B) Size of BP-L measured by DLS.

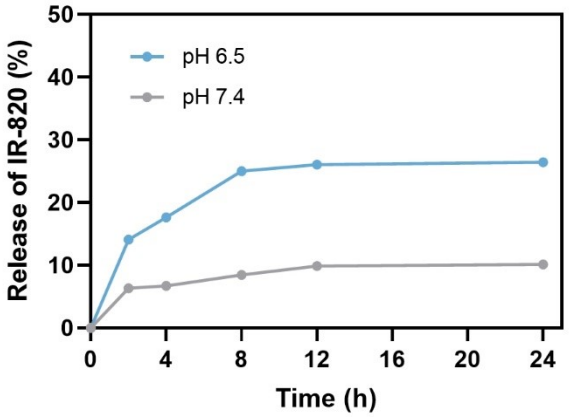

Figure S2. IR-820 release curve of IR@BP-L in different pH (6.5, 7.4).

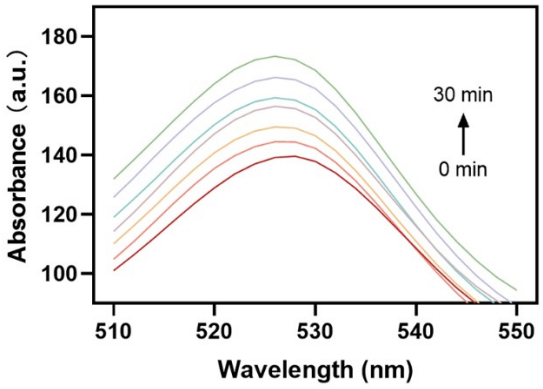

Figure S3. Evaluation of ROS production by IR@BP-L under 808 nm laser through detecting UV-vis absorption of DCF from 510 nm to 550 nm. The ROS generation was quantitatively calculated by the adsorption value at 529 nm.

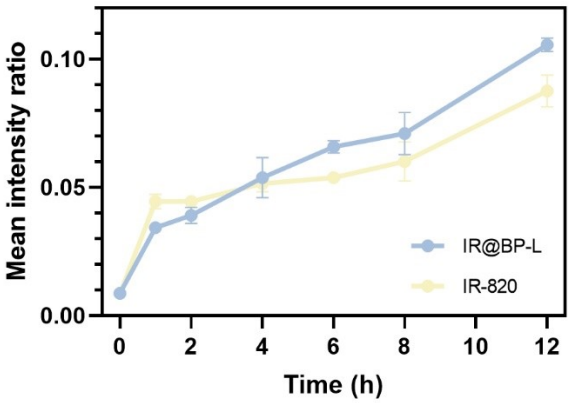

Figure S4. Quantitative analysis of cellular uptake by CLSM. Data are presented as mean ± SEM (n = 3).

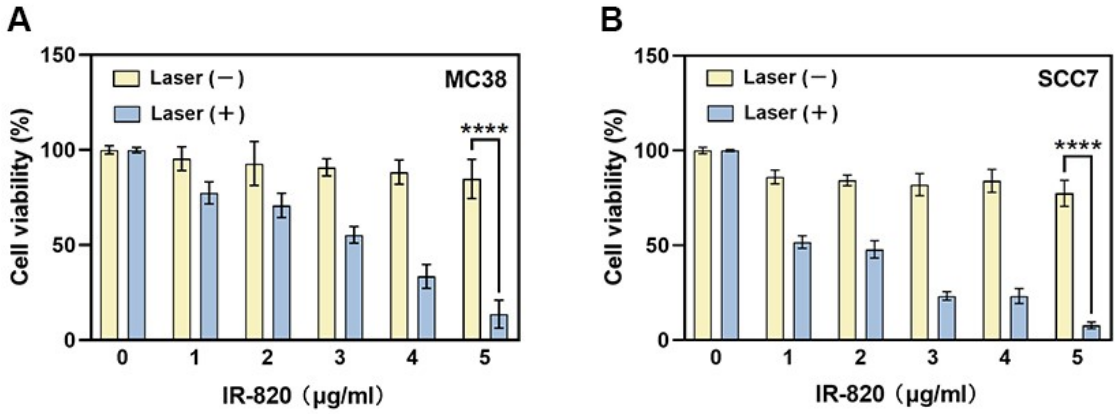

Figure S5. Cytotoxicity of (A) MC38 and (B) SCC7 cells with IR-820. Data are presented as mean ± SEM (n = 4). ****p < 0.0001, respectively.

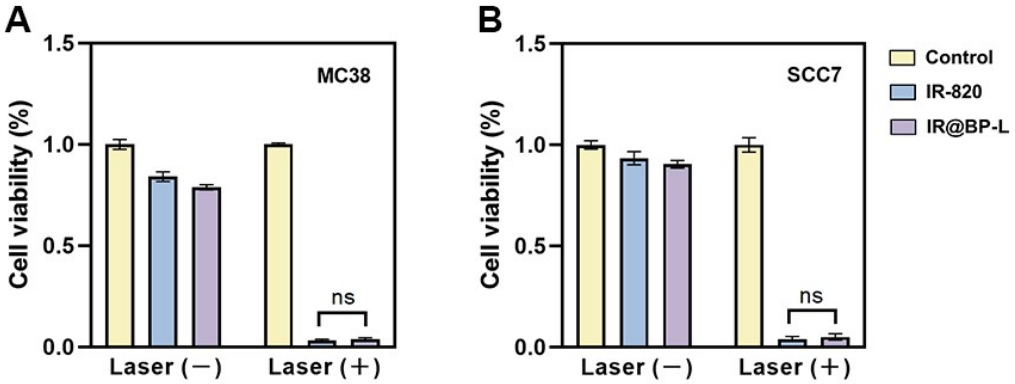

Figure S6. Cytotoxicity of IR-820 and IR@BP-L (IR-820, 5 ug/mL) in (A) MC38 and (B) SCC7 cells. Data are presented as mean ± SEM (n = 4). Ns represents no significance, respectively.

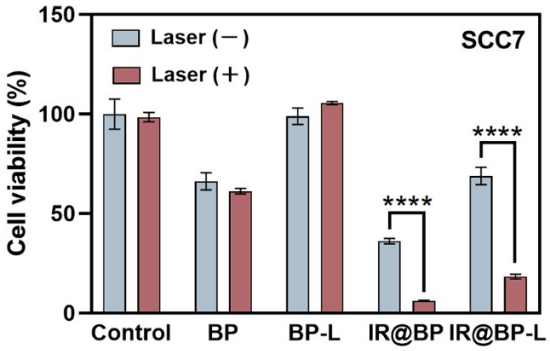

Figure S7. Cytotoxicity of SCC7 cells with different treatment groups. Data are presented as mean ± SEM (n = 4). ****$p < 0.0001$, respectively.

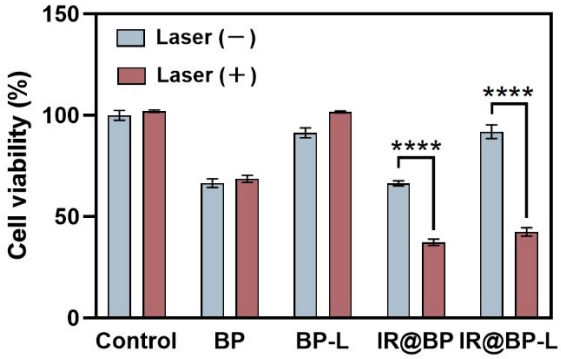

Figure S8. Quantitative analysis of Live/dead staining. Data are presented as mean ± SEM (n = 3).

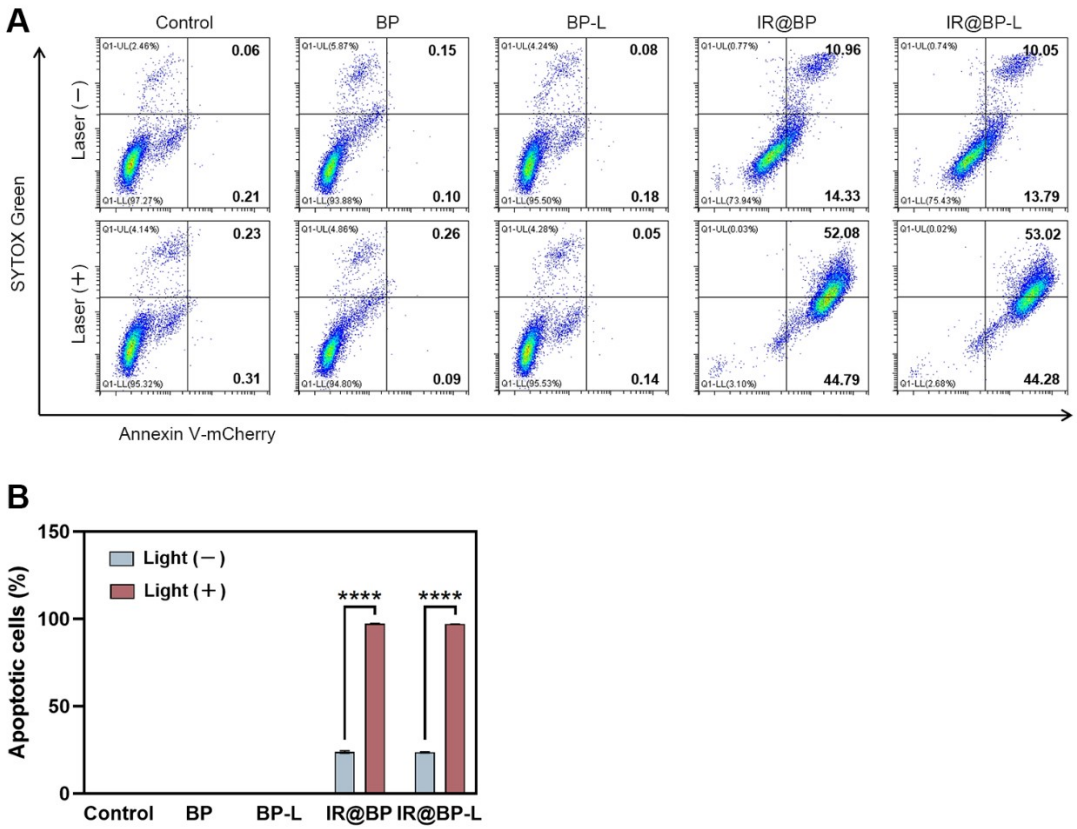

Figure S9. (A) Representative flow cytometry plots and (B) quantitative analysis of apoptotic SCC7 cells with Annexin V-mCherry/SYTOX Green staining. Data are presented as mean ± SEM (n = 3). ****$p < 0.0001$, respectively.

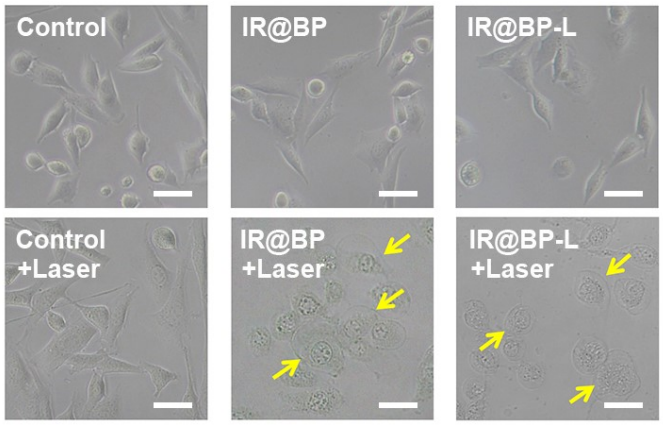

Figure S10. Representative microscopy images of SCC7 cells treated with different treatments. The pyroptosis cells were indicated by yellow arrows. Scale bar: 25 μm.

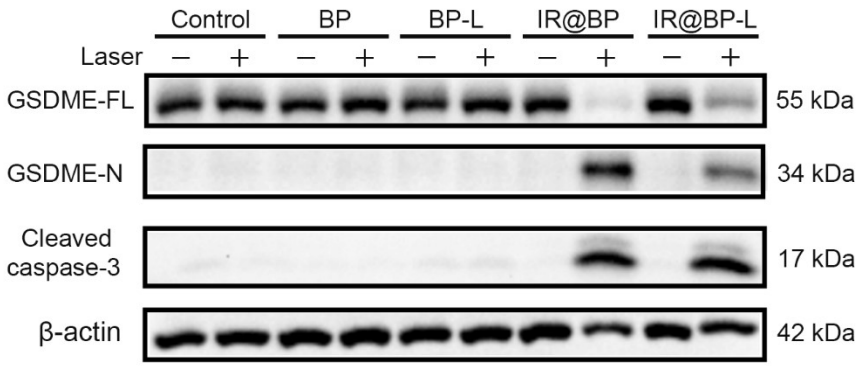

Figure S11. The expression of GSDME-FL, GSDME-N, and cleaved caspase-3 in SCC7 cells with different treatments.

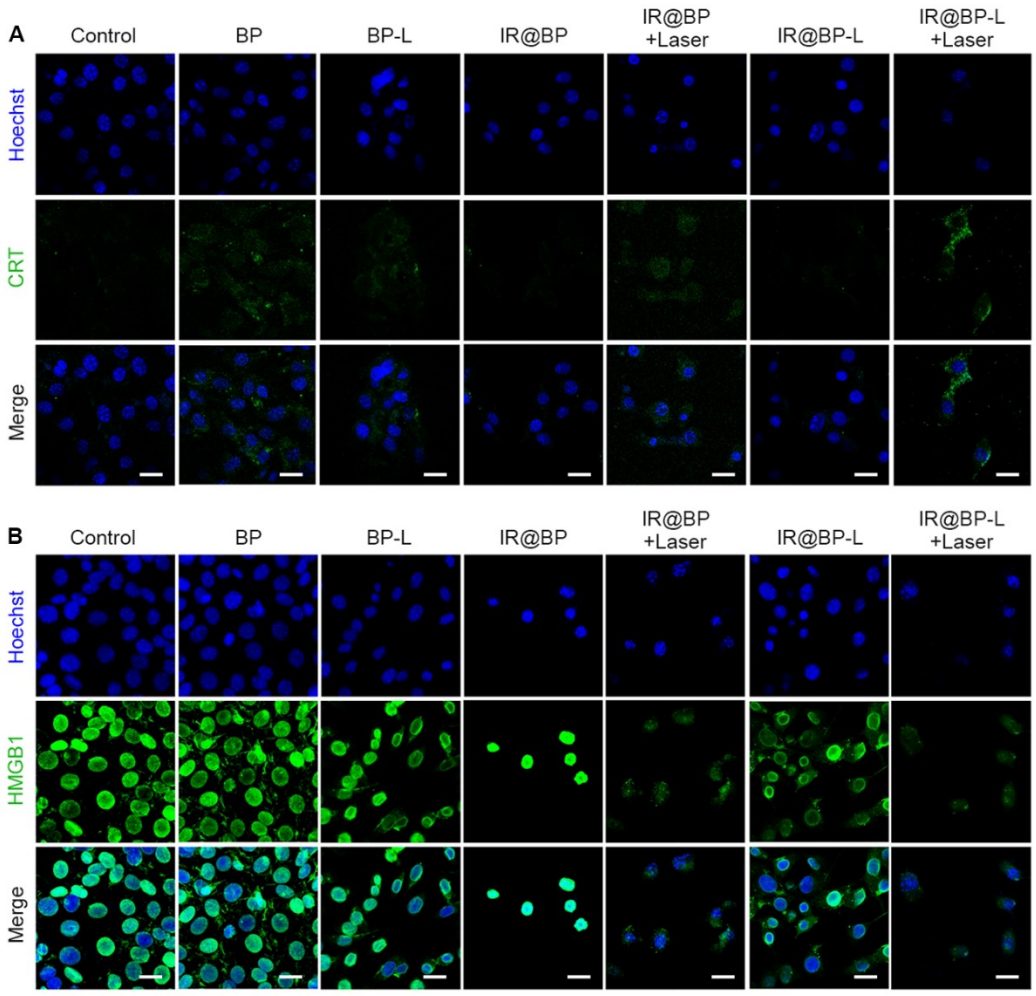

Figure S12. Representative fluorescent images of (A) CRT and (B) HMGB1 in SCC7 cells. Scale bar: 20 μm.

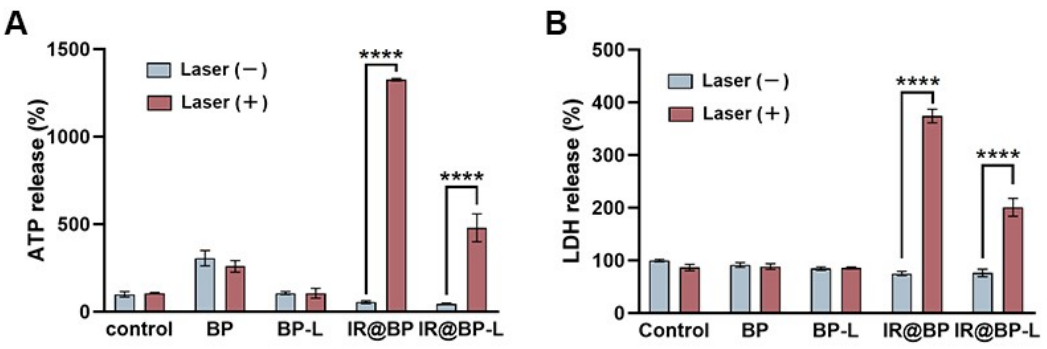

Figure S13. Release levels of (A) ATP and (B) LDH from SCC7 cells in different treatment groups. Data are presented as mean ± SEM (n = 3). ****p < 0.0001, respectively.

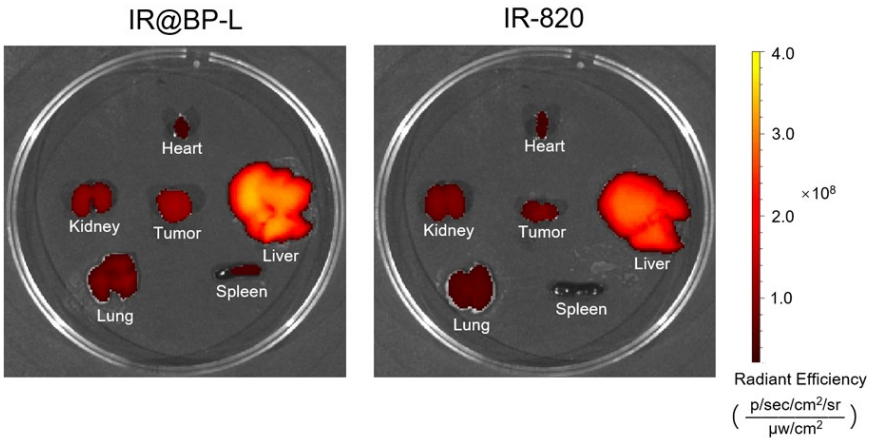

Figure S14. Representative *ex vivo* fluorescence images of major organs and tumors isolated from mice at 24 h post i.v. injection of IR@BP-L and IR-820.

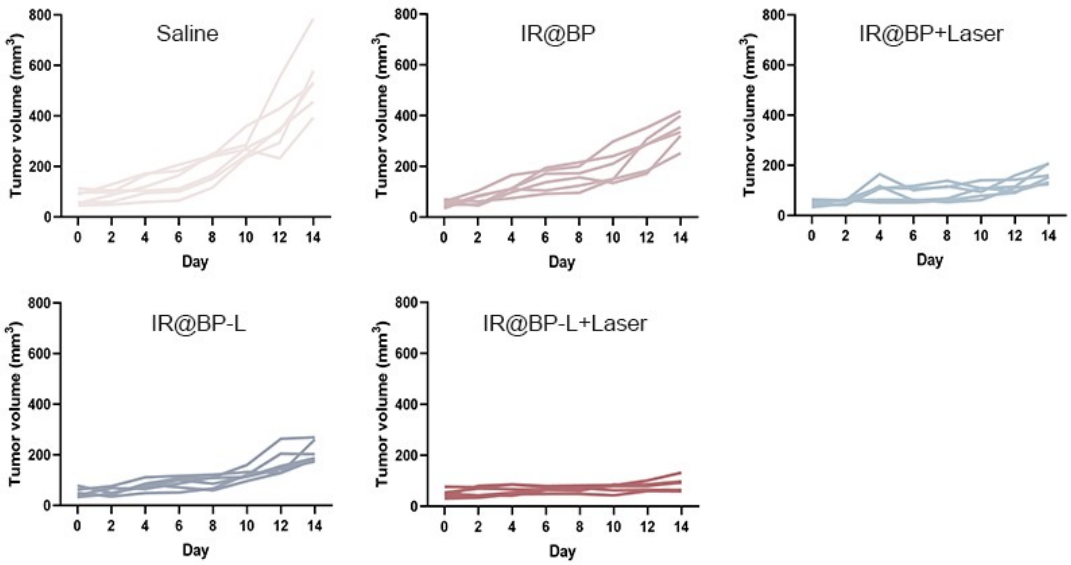

Figure S15. Individual growth curves in different treatment groups (n = 6).

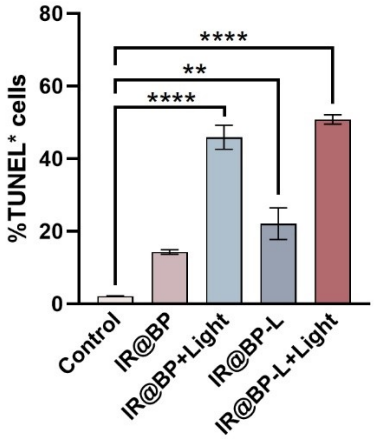

Figure S16. Quantification of TUNEL positive cells. Data are presented as mean ± SEM (n = 3). **p < 0.01, ***p < 0.001, and ****p < 0.0001, respectively.

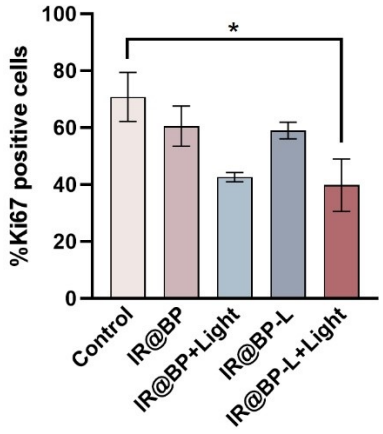

Figure S17. Quantification of Ki67 positive cells. Data are presented as mean ± SEM (n = 3). *p < 0.05, respectively.

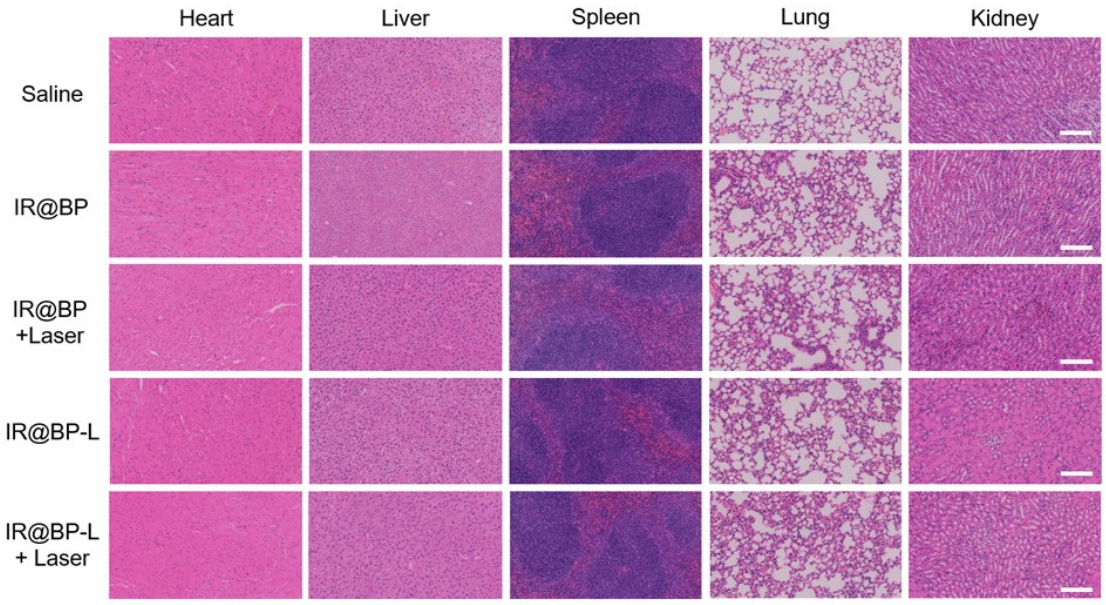

Figure S18. Representative H&E staining images of the major organs (heart, liver, spleen, lung, and kidney) of mice from different treatment groups. Scale bar: 50 μm.

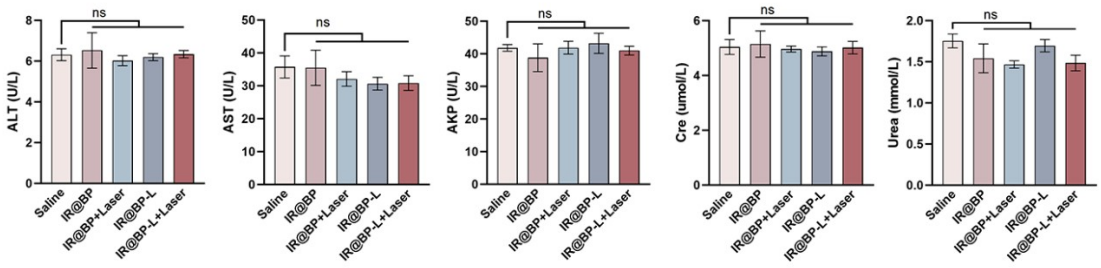

Figure S19. The ALT, AST, AKP, cre and urea levels in the serum of mice from different treatment groups. Data are presented as mean ± SEM (n = 5). Ns represents no significance, respectively.

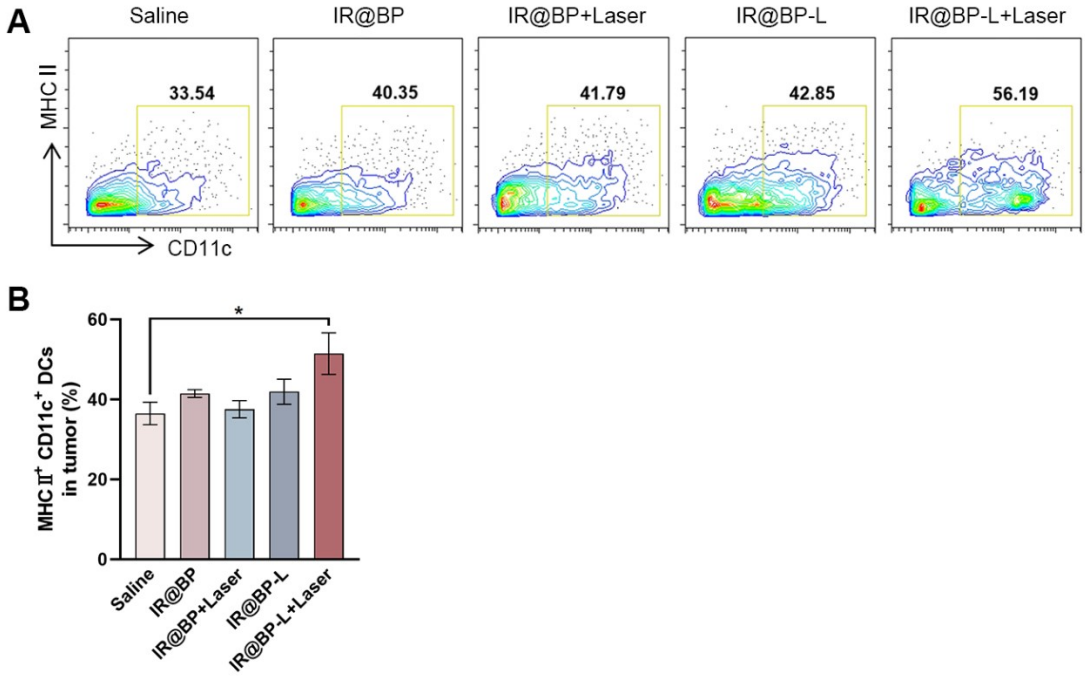

Figure S20. Representative flow cytometry plots and quantitative analysis of MHCII$^+$/CD11c$^+$ DCs in the tumors of mice from different treatment groups. Data are presented as mean ± SEM (n = 3). *p < 0.05, respectively.

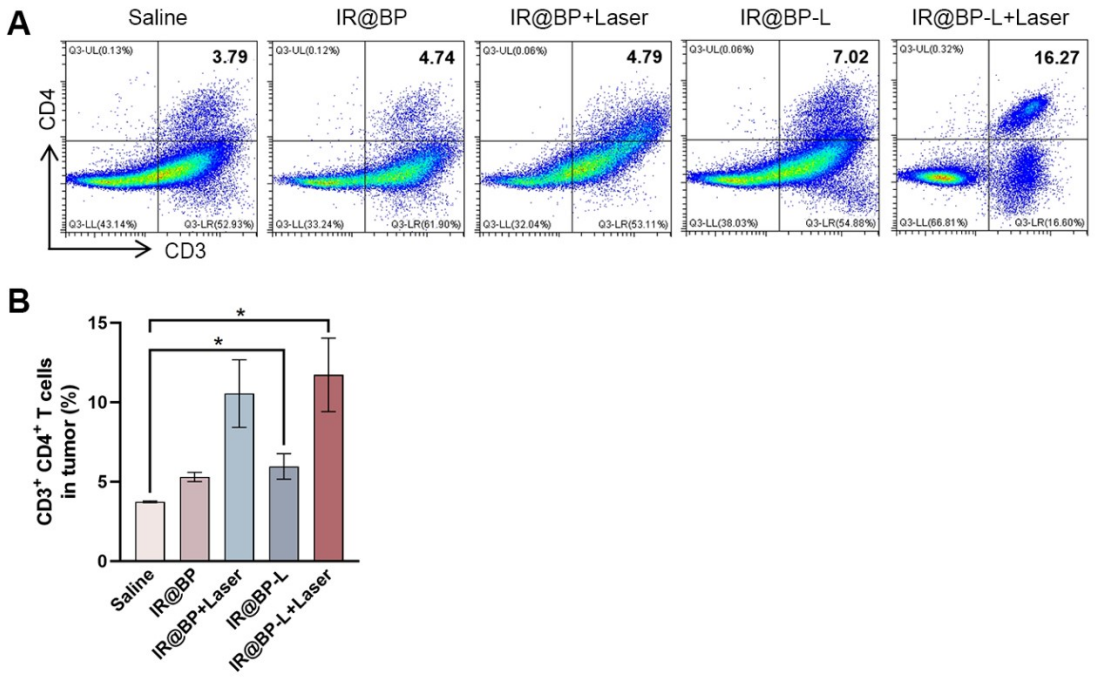

Figure S21. Representative flow cytometry plots and quantitative analysis of $CD3^+/CD4^+$ T cells in the tumors of mice from different treatment groups. Data are presented as mean ± SEM (n = 3). *$p < 0.05$, respectively.

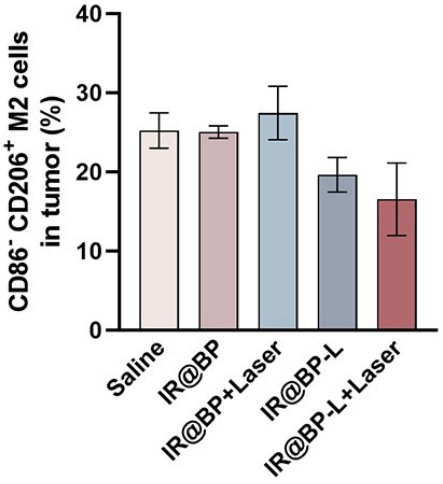

Figure S22. Quantitative analysis of $CD86^-/CD206^+$ M2 macrophages in the tumors of mice from different treatment groups. Data are presented as mean ± SEM (n = 3).